# STERICALLY CROWDED HETEROCYCLES. XI. A SEMIEMPIRICAL PREDICTION OF ENANTIOMERIZATION BARRIERS FOR SUBSTITUTED (*Z*)-3-(IMIDAZO[1,2-*a*]PYRIDIN-3-YL)-1-PHENYLPROP-2-EN-1-ONES

Stanislav BÖHM[1,*], Radek POHL[2] and Josef KUTHAN[3]

*Department of Organic Chemistry, Prague Institute of Chemical Technology, 166 28 Prague 6, Czech Republic; e-mail: [1] stanislav.bohm@vscht.cz, [2] radek.pohl@vscht.cz, [3] josef.kuthan@vscht.cz*

Received May 21, 1999
Accepted August 27, 1999

*Dedicated to Professor Otto Exner on the occasion of his 75th birthday.*

Conformational behaviour and racemization paths of the parent skeleton are discussed using a threedimensional Φ,Ψ-energy map calculated by the semiempirical PM3 method. To restrain the number of possible racemization paths, a less sophisticated approach based on the PM3 heat of formation – torsion angle Φ relationships has been used for 5-substituted title molecules; the role of non-planar enantiomeric transition states is postulated. Plausibility of the simple theoretical procedure has been tested using two phenyl derivatives of the title compounds for which experimental barriers to racemization are accessible.

**Key words**: Imidazo[1,2-*a*]pyridines; Axial chirality; Transition states; PM3 method; Rotation barriers; Hindered rotation; Atropisomerism; Semiempirical calculations.

The extended Decker oxidation[1] of appropriate quaternary 1,4-disubstituted 2,6-diarylpyridinium salts has been shown[2] to be a simple stereospecific approach to various crowded α,β-unsaturated ketones of (*Z*)-configuration with respect to corresponding imidazo[1,2-*a*]heteroarene moieties. Compounds **1** and **2** are typical examples of the products; investigations of the parent derivative **1a** using chiral NMR shift reagents[2b], X-diffraction analysis[2c] and semiempirical PM3 calculations[2c] really predict atropisomerism for **1**- and **2**-like molecules due to a restricted rotation around the 3,3′-bond. Meanwhile, a newly developed[3] chiral HPLC procedure using polarimetric detection has been also applied[3c] to indicate enantiomeric instability of the parent **1a** and to determine the racemization Gibbs energies $\Delta G^{\neq}$ for alcoholic solutions of compounds **1b** and **1c**. The experimental data stimulate us to consider reliability of theoretical barriers to racemization calculated by the semiempirical PM3 method[4a,4b] for a more

extended series of related axially chiral compounds **1a**–**1g** and **2a**–**2g**. They were – except for **2g** – synthesized[5] but the corresponding experimental barriers are not available or hardly obtainable by the mentioned online method[3] because of their too high values. The results of theoretical treatment are presented in this paper.

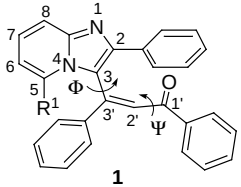


**1**

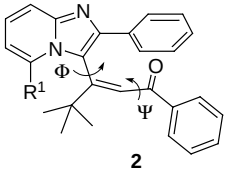


**2**

| **1-2** | **a** | **b** | **c** | **d** | **e** | **f** | **g** |
|---|---|---|---|---|---|---|---|
| $R^1$ | H | Ph | Me | Et | Bu | i-Pr | *t*-Bu |

## CALCULATIONS

Considering the size of the studied molecular systems **1a**–**2g**, any *ab initio* method has been avoided for the present; instead, the standard semiempirical PM3 procedure[4a] was therefore used for all calculations. Full molecular energy optimizations for fixed values of the angle Φ or for both fixed angles Φ and Ψ were stepwise calculated (every step after 10° change). Some of the PM3 calculated characteristics are given in Table I. Other molecular energy relationships can be also seen in the 3D diagram (Fig. 1) which was obtained from 1 369 SCF energy values calculated for PM3 models of the molecule **2a** and by a cartographic procedure[4d]. As a starting point in all calculations, one arbitrary molecular geometry optimized with respect to all degrees of freedom by the standard MM2 procedure[4c] has been used for a given molecule.

## RESULTS AND DISCUSSION

A theoretical prediction of energy barriers to racemization does not seem to be a trivial task for such sterically hindered molecules as **1a**–**1g** and **2a**–**2g**. Hence, an approximate but practically useful approach based on the semiempirical PM3 method[4a,4b] has been developed. This follows from the preceding work[2c] in which conformational behaviour of the molecule **1a** has been investigated using a PM3 calculated Φ,Ψ-energy map but obtaining at least four possible racemization barriers in the range from 13.5 to 23.5 kcal/mol given by rotation about the C3–C3′ bond. A similar conform-

ational behaviour may be expected for other **1**-like molecules. On the other hand, it seems desirable to investigate how side chain 3′-*tert*-butyl group in the **2**-like molecules affects their conformational properties; therefore, the same PM3 procedure has been applied to analogous derivative **2a**. From Fig. 1 it can be concluded that the PM3 conformational model of **2a** resembles, to a considerable extent, that reported[2c] for the 3′-phenyl derivative **1a**. The resulting 3D contour surface contains two very flat (*S*)- and (*R*)-areas involving numerous conformations of the enantiomeric (*S*)- and (*R*)-molecules. These areas are separated by energy "mountain" ridges with several saddles suggesting possible paths to racemization and indicating that the restricted rotation around the C3–C3′ bond characterized by changes in the torsion

TABLE I
Calculated racemization barriers (in kcal/mol) and torsion angles (in °, ±5°). See text for definitions

| $R^1$ | $\Delta E_1$ | $\Delta E_2$ | $\delta\Delta H_f$ | $\Phi_S$ | $\Phi_{ATS1}$ [a] | $\Phi_{ATS2}$ [a] |
|---|---|---|---|---|---|---|
| | | | **1a–1g** | | | |
| H | 13.8 | 16.3 | +2.5 | 80 | 10 | 180 |
| Ph[b] | 27.1 | 17.7 | +0.3 | 80 | 40 | 200 |
| Me[c] | 28.4 | 22.9 | –1.9 | 90 | 40 | 190 |
| Et | 31.0 | 26.5 | –1.1 | 90 | 40 | 190 |
| Bu | 30.6 | 26.4 | –0.1 | 80 | 40 | 200 |
| i-Pr | 30.0 | 26.2 | –1.0 | 100 | 40 | 200 |
| *t*-Bu | 25.4 | 29.7 | –1.5 | 70 | 50 | 200 |
| | | | **2a–2g** | | | |
| H | 30.0 | 31.9 | +1.7 | 100 | 10 | 190 |
| Ph[b] | 47.4 | 42.2 | +0.8 | 100 | 30 | 220 |
| Me[c] | 40.1 | 43.9 | –1.1 | 80 | 30 | 200 |
| Et | 38.8 | 42.9 | –2.1 | 80 | 40 | 200 |
| Bu | 55.5 | 45.7 | –0.7 | 110 | 40 | 230 |
| i-Pr | 43.7 | 42.7 | –1.7 | 80 | 45 | 200 |
| *t*-Bu | 43.6 | 42.3 | –1.6 | 110 | 30 | 230 |

[a] For a Φ-change in the direction from 0 to 360°. [b] Experimental data (MeOH, 40 °C, ref.[3c]): $\Delta G^{\neq}$ = 24.4 kcal/mol, $t_{0.5}$ = 101 min. [c] Experimental data (EtOH, 60 °C, ref.[3c]): $\Delta G^{\neq}$ = 26.1 kcal/mol, $t_{0.5}$ = 118 min.

angle Φ is really responsible for the axial chirality of the parent **2a** and, consequently, also for related molecules **2b**–**2g**. To simplify estimation of the racemization barriers, the following procedure has been used: In the first step, a molecular conformation for an angle Φ inside the (*S*)-area – estimated by preliminary MM2 calculations – was PM3-optimized with respect to all degrees of freedom and thus the calculated molecular geometry and an appropriate heat of formation $\Delta H_f$(start) were the starting points from which the other $\Delta H_f$ values were obtained by stepwise changes of the Φ-angles from 0 to 360°. In every step, optimization with respect to all geometry degrees of freedom, except for the fixed torsion angle Φ, was performed. Typical $\Delta H_f = f(\Phi)$ curves obtained for the isomeric PM3 models of **1g** and **2b** are shown in Fig. 2. Similarly, to those for all remaining PM3 models of

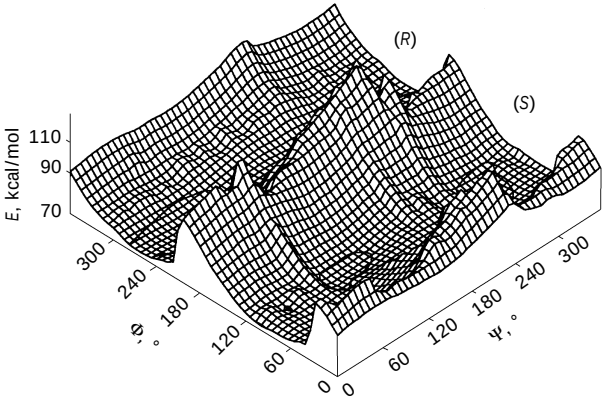


FIG. 1
3D molecular Φ,Ψ-energy diagram for the molecule **2a** based on the PM3 heats of formation and calculated for the direction 0 to 360°

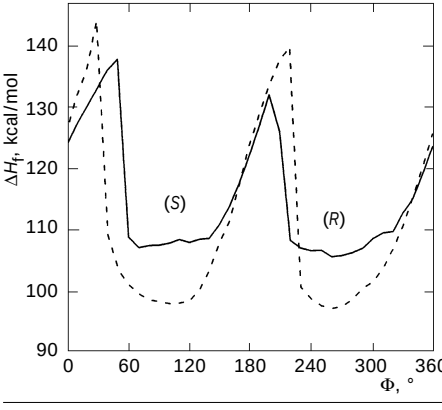


FIG. 2
Dependences of the PM3-calculated heats of formation $\Delta H_f$ for the isomeric derivatives **1g** (—) and **2b** (----) on the torsion angles Φ

**1a**–**1f**, **2a** and **2c**–**2g**, they exhibit two minima, $\Delta H_f(S)$ and $\Delta H_f(R)$ and two different energy maxima, $\Delta H_f$(ATS1) and $\Delta H_f$(ATS2) assigned to two approximate conformational transition states ATS1 and ATS2 corresponding to two racemization paths shown in Scheme 1. The enantiomeric relationship between the both minima has been tested by visualization of the corre-

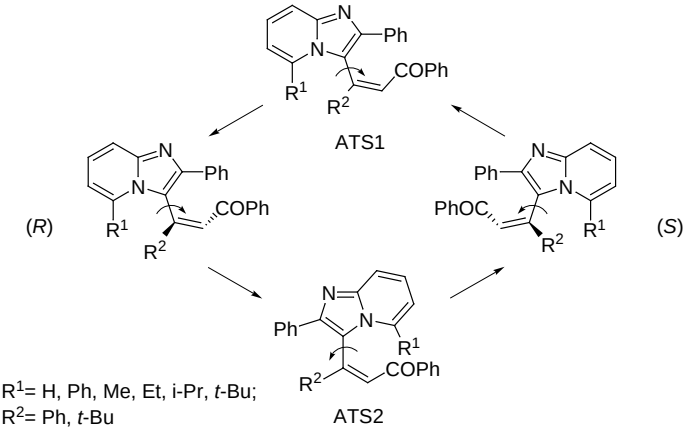


SCHEME 1

sponding molecular geometries as exemplified for **2b** in Fig. 3. It is obvious that the two minima really correspond to entirely mirror (*S*)- and (*R*)-conformations. Because their calculated molecular geometries are slightly different, the inaccuracy in their heats of formations $\Delta H_f(R)$ and $\Delta H_f(S)$ may be

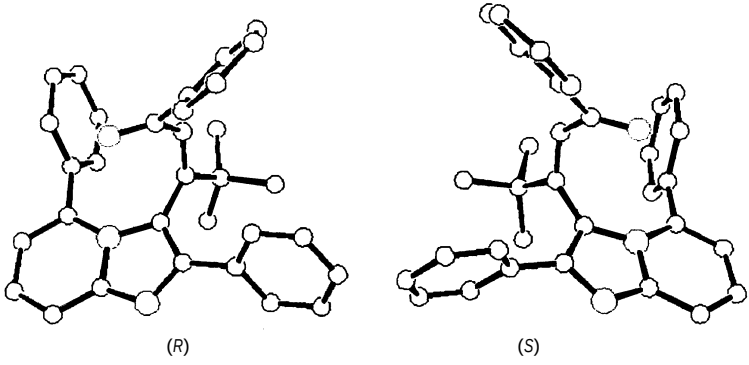


FIG. 3

PM3-Calculated molecular structures (hydrogen atoms are omitted) of the enantiomer (*R*)-**2b** corresponding to the first minimum (left) and of the enantiomer (*S*)-**2b** corresponding to the second minimum (right) on the $\Delta H_f = f(\Phi)$ curve (----) shown in Fig. 2

expected within the values $\delta\Delta H_f = \Delta H_f(R) - \Delta H_f(S)$. As follows from Table I, the latter values do not usually exceed the range of *ca* ±2.5 kcal/mol.

To overcome the problem of the somewhat different energy barriers, we have decided to represent their "improved" energy values by the arithmetic averages $\Delta E_1 = \Delta H_f(\text{ATS1}) - [\Delta H_f(R) + \Delta H_f(S)]/2$ and $\Delta E_2 = \Delta H_f(\text{ATS2}) - [\Delta H_f(R) + \Delta H_f(S)]/2$. The corrected data are also given in Table I.

Thus, using the approximate approach, the occurrence of both ATS1 and ATS2 makes it possible to describe the racemization process just by two easily calculated barriers to rotation and two pathways shown in Scheme 1.

A real existence of the both TS's was proved by vibrational analysis showing only one imaginary frequency in every case. Comparable participations of all degrees of freedom in the geometry changes follows from the transition vector analysis. This fact is also reflected, to a certain degree, in the later discussed "saw tooth" fashion of the studied $\Delta H_f = f(\Phi)$ curves due to a large cumulation of intramolecular steric strain, within a relatively broad region of the angles Φ, followed by a sudden molecular relaxation when the absolute configuration is changed. This is even more remarkable if smaller steps for the Φ changes are applied in the relaxation region.

We have, however, found that the shapes of the energy barriers as well as the $\Phi_{ATS1}$ and $\Phi_{ATS2}$ angles depend upon the direction of rotation forwards (Φ: 0 → 360°) or backwards (Φ: 360 → 0°). All the investigated $\Delta H_f = f(\Phi)$ curves for **1a**–**1g** and **2a**–**2g** exhibit a typical "saw tooth" effect consisting in a progressive energy increase up to the maximum and a sharp drop to the next minimum as illustrated for the derivative **2b** in Fig. 4. In addition, the slope of the barriers is invariably lower from the direction of changing the angle Φ. The feature has been also observed[6,7] in some other AM1 and

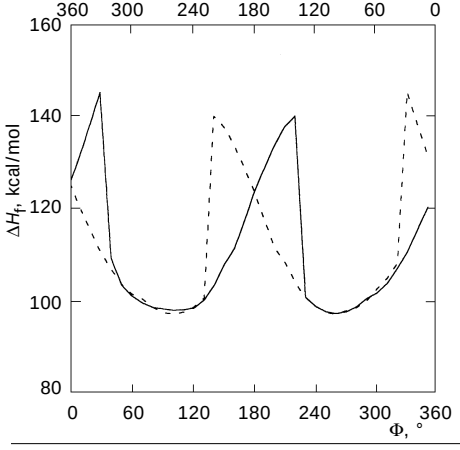


FIG. 4
Demonstration of the "saw tooth" effect on the $\Delta H_f = f(\Phi)$ curves obtained by the directions of rotation 0 → 360° (—) and 360 → 0° (----) for the molecule **2b**

PM3 calculations on larger inherently hindered molecules and attributed to relaxation given by distortion of the pyrazine ring[6] in the molecule **4** or the fused (hetero)aromatic systems[7] in the molecule **5**. In fact, a pyramidal – coplanar configuration change at the N(4) nitrogen centre can be also seen in the PM3 conformations of the molecules **1** and **2** after the sharp energy drops.

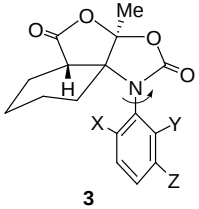


**3**

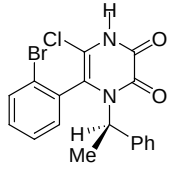


**4**

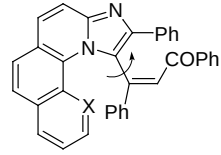


**5**

It may be noted that a similar two-barrier system has been assumed[8] purely speculatively for the interconversion between **3**-type rotamers where, however, only the pathway *via* a lower-energy TS has been considered. Similarly, only one lower-energy AM1-calculated barrier for the enantiomerization of the sterically hindered 6-arylpyrazinone derivative **4** has been considered recently[6]. As it follows from Table I, in the case of the 5′-unsubstituted compound **2a**, the PM3-calculated barriers to rotation are comparable and therefore both have to be taken into account. In fact, it is evidently the case for most of the other molecules investigated in this paper.

The calculated Φ-values for the energy extremes for the rotation in the direction 0 to 360° (Table I) and the molecular shapes given in Figs 3 and 5

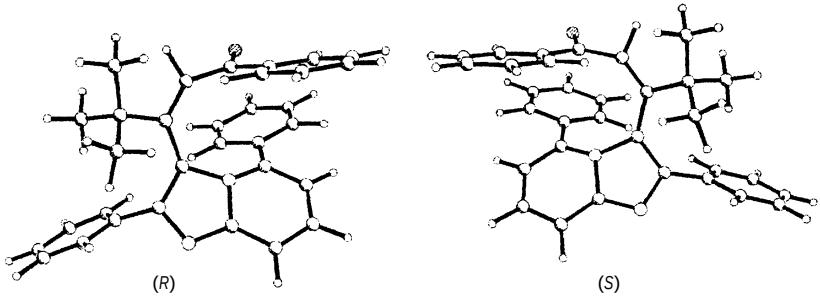


FIG. 5

PM3-Calculated structures of the rotation transition states ATS2 calculated for the molecular system **2b** (Fig. 2) in the directions 0 → 360° (left) and 360 → 0° (right)

show that neither in the (*S*)- and (*R*)-conformers nor in the ATS1 and ATS2 states, the side chain –C=C–COPh is coplanar with the imidazo[1,2-*a*]-pyridine ring system due to the sterically crowded nature of all conformations of the molecules. In addition, the $\Delta H_f = f(\Phi)$ curves do not reach their maxima at the angles $\Phi$ = 0, 180 and 360° for which the diene fragment C(2)=C(3)–C(3′)=C(2′) is planar. Hence, the atropisomeric **1**- and **2**-like molecules change their absolute configurations even before they overcome the corresponding energy barrier. This may be understandable since the sterically crowded arrangement within the molecular moieties hinders them to adopt totally planar TS conformations. Whereas the $\Delta H_f$(ATS1) and $\Delta H_f$(ATS2) values are independent of the direction of rotation, this is unfortunately not the case of the corresponding angles $\Phi_{ATS1}$ and $\Phi_{ATS2}$ leading to enantiomeric ATS1 and ATS2 as illustrated for one of them in Fig. 5.

Owing to the above demonstrated existence of both ATS1 and ATS2 based on their full geometry optimizations starting from a given $\Delta H_f = f(\Phi)$ curve and completed by vibration analysis, it may be concluded that the observed direction effects on the curves is probably not the computational artifact known as chemical hysteresis. A detailed study of multidimensional hypersurface is out of scope of this study and may be also hardly feasible by the PM3 semiempirical method. This question remains to be open for a future study using MD and more sophisticated MO methods.

As follows from Table I, both the predicted rotation barriers, $\Delta E_1$ and $\Delta E_2$, differ no more than 4 kcal/mol for most of the studied examples except for the cases **1b** ($R^1$ = Ph), **1g** ($R^1$ = *t*-Bu), **2b** ($R^1$ = Ph) and **2e** ($R^1$ = Bu) where one of the paths is apparently preferred and the racemizations might proceed almost exclusively *via* the lower ATS. On the other hand, a comparison of experimental $\Delta G^{\neq}$ data, 24.4 and 26.1 kcal/mol, obtained[3c] for alcoholic solutions of methyl and phenyl derivatives **1b** and **1c** with the corresponding $\Delta E_{1,2}$ values 17.7, 27.1 and 22.9, 28.4 kcal/mol (Table I) suggests that the racemizations probably proceed *via* both the pathways at least in solution provided solvent effects are small. In fact, it is probably the case for most axially chiral substances since non-negligible effects of solvation have been rarely observed[9]. In addition, the calculated lower $\Delta E_{1,2}$ energies, 16.3 and 13.8 kcal/mol, for the parent compound **1a** are in agreement with the observed[3c] lower enantiomeric stability of the substance in solution.

The data in Table I also demonstrate a more retarding steric effect of the 3′-*tert*-butyl group in the molecules **2b**–**2g** ($\Delta E_{1,2}$ = 38.8–55.5 kcal/mol) compared with that of the 3′-phenyl substituent in the molecules **1b**–**1g**

($\Delta E_{1,2}$ = 17.7–31.2 kcal/mol). Hence, it may be predicted that the former compounds hardly racemize at usually accessible temperatures in agreement with our aquired experience.

## CONCLUSION

Apart from a limited accuracy of the presented semiempirical data, the atropisomerism of imidazo[1,2-*a*]pyridine derivatives **1a**–**1g** and **2a**–**2g** can be characterized in depth by the PM3-calculated energy rotation barriers $\Delta E_{1,2}$. It may be expected that related molecules possessing *Z*-configuration at the C3–C3′ bond will exhibit a similar stereochemical behaviour especially for the bulky 3-substituents.

*The authors would like to express their thanks to Prof. A. Mannschreck, Institute of Organic Chemistry, University of Regensburg, Germany for valuable discussion and some original experimental data. This work was sponsored by the Grant Agency of the Czech Republic (grant No. 203/96/0497).*

## REFERENCES

1. Kuthan J.: *Heterocycles* **1994**, *37*, 1347.
2. a) Böhm S., Kubík R., Novotný J., Ondráček J., Kratochvíl B., Kuthan J.: *Collect. Czech. Chem. Commun.* **1991**, *56*, 2326; b) Kubík R., Němeček J., Böhm S., Hradilek M., Kuthan J.: *Mendeleev Commun.* **1995**, 29; c) Böhm S., Kubík R., Hradilek M., Němeček J., Hušák M., Kratochvíl B., Kuthan J.: *Collect. Czech. Chem. Commun.* **1995**, *60*, 115.
3. a) Mannschreck A.: *Chirality* **1992**, *4*, 163; b) Mannschreck A., Schinabeck M., Brandl F.: *Chem. Listy* **1998**, *92*, 261; c) Mannschreck A., Pustet N.: Unpublished results.
4. a) Stewart J. J. P.: *J. Comput. Chem.* **1989**, *10*, 209; b) Stewart J. J. P.: J. *Comput. Chem.* **1989**, *10*, 221; c) *Program CS Chem 3D Pro Version 3.5.1*. Cambridge Soft Corporation, Cambridge (MA) 1996; d) *Program Surfer Version 5.00*. Golden Software, Golden (CO) 1994.
5. a) Kubík R., Böhm S., Havlíček V., Strnad T., Kratochvíl B., Kuthan J.: *Collect. Czech. Chem. Commun.* **1996**, *61*, 1473; b) Pohl R., Böhm S., Kuthan J.: *Collect. Czech. Chem. Commun.* **1999**, *64*, 1274.
6. Tulinsky J., Cheney B. V., Mizsak S. A., Watt W., Han F., Dolak L. A., Judge T., Gammill R. B.: *J. Org. Chem.* **1999**, *64*, 93.
7. Böhm S., Strnad T., Ruppertová I., Kuthan J.: *Collect. Czech. Chem. Commun.* **1997**, *62*, 1599.
8. Saito K., Yamamoto M., Yamada K.: *Tetrahedron* **1993**, *49*, 4549.
9. Cox C., Lectka T.: *J. Org. Chem.* **1998**, *63*, 2426.